

# Cobalt Nanoparticle Formation in the Pores of Hyper-Cross-Linked Polystyrene: Control of Nanoparticle Growth and Morphology

S. N. Sidorov, L. M. Bronstein,\* V. A. Davankov, M. P. Tsyurupa, S. P. Solodovnikov, and P. M. Valetsky

*Nesmeyanov Institute of Organoelement Compounds, 28 Vavilov St., Moscow 117813, Russia*

E. A. Wilder and R. J. Spontak

*Departments of Chemical Engineering and Materials Science & Engineering, North Carolina State University, Raleigh, North Carolina 27695*

*Received May 6, 1999. Revised Manuscript Received August 26, 1999*

Impregnation of hyper-cross-linked polystyrene (HPS) by either  $\text{Co}_2(\text{CO})_8$  in 2-propanol or the  $[\text{Co}(\text{DMF})_6]^{2+}[\text{Co}(\text{CO})_4]^{-2}$  complex in dimethylformamide (DMF), followed by thermolysis at 200 °C, results in the formation of discrete Co nanoparticles. The concentration and characteristics of such nanoparticles were investigated by X-ray fluorescence (XRF) spectroscopy, ferromagnetic resonance (FMR) spectroscopy, and transmission electron microscopy (TEM). The FMR data here confirm the formation of spherical nanoparticles. At relatively low concentrations of Co, the magnitude of the FMR line width reveals that the mean Co nanoparticle diameter is about 2 nm, which agrees closely with the mean particle diameter discerned by TEM. An increase in Co content higher than 8 wt % is accompanied by an increase in mean particle diameter due to an increase in the population of large Co nanoparticles up to 15 nm across. Regulated nanoparticle growth over a wide range of Co concentrations is attributed to nanoscale HPS cavities, which serve to physically restrict the size of growing particles.

## Introduction

Nanoscale metal and metal oxide (or sulfide) particle preparation remains a topic of tremendous interest due principally to the unique properties displayed by materials containing such particles. Due to the nanometer size of these particles, their physicochemical characteristics differ significantly from those of molecules and bulk materials.<sup>1</sup> Particle properties of technological relevance include, but are not limited to, catalytic, semiconductor, magnetic, and optical properties, each of which could be applied to various topics in physics, chemistry, and materials science.<sup>1–3</sup> The formation of such nanoparticles necessarily requires, however, stabilization to prevent agglomeration, which would eradicate most of their desirable advantages relative to bulk materials of identical composition. While contemporary preparation techniques permit the formation of nano-sized metals through the use of a wide range of stabilizing agents,<sup>1</sup> the use of organic polymers as environments for in situ nanoparticle growth would synergistically combine the properties of both the host polymeric matrix and the discrete nanoparticles formed therein.

The most advanced, yet relatively simple, method by which to prepare solid-state composite materials possessing nanoparticles begins with the introduction of an organometallic compound into a polymeric matrix, followed by hydrolysis, thermolysis, or some other means of reducing the metal species. Thermolysis of  $\text{Co}_2(\text{CO})_8$ , for instance, has been successfully employed<sup>4–6</sup> to produce Co nanoparticles in a variety of polymeric matrixes. An interesting observation in these studies is that the type of polymer matrix plays an important role in Co nanoparticle formation by controlling the size, shape, and, hence, properties of the resultant nanoparticles. Similar routes have been explored<sup>7–10</sup> for the preparation of a wide range of transition-metal nanoparticles in different polymer matrixes.

Metal nanoparticles may also be synthesized in lightly cross-linked polymer gels.<sup>11,12</sup> Due to the intrinsic polydispersity of pore sizes in gels, however, it is virtually impossible to ensure fine control over nano-

\* To whom correspondence should be addressed at the Department of Chemistry, Indiana University, Bloomington, IN 47405. Telephone: (812) 855-6971. Fax: (812) 855-8300. E-mail: lybronst@indiana.edu.

(1) Schmid, G. *Clusters and Colloids*; VCH: Weinheim, 1994.  
(2) Fendler, J. H. *Nanoparticles and Nanostructured Films*; Wiley-VCH: Weinheim, 1998.  
(3) Henglein, A. *Chem. Rev.* **1989**, *89*, 1861.

(4) Bronstein, L. M.; Mirzoeva, E. Sh.; Seregina, M. V.; Valetsky, P. M.; Solodovnikov, S. P.; Register, R. A. In *Nanotechnology, Molecularly Designed Materials*; Chow, G.-M., Gonsalves, K. E., Ed.; American Chemical Society: Washington, DC, 1996.

(5) Thomas, J. R. *J. Appl. Phys.* **1966**, *39*, 2914.  
(6) Hess, P. H.; Parker, P. H. *J. Appl. Polym. Sci.* **1966**, *10*, 1915.  
(7) Yamato, H.; Koshihara, T.; Ohwa, M.; Wernet, W.; Matsumura, M. *Synth. Met.* **1997**, *87*, 231.  
(8) Chen, L.; Liu, K.; Yang C. Z. *Polym. Bull.* **1996**, *37*, 377.  
(9) Troger, L.; Hunnefeld, H.; Nunes, S.; Oehring, M.; Fritsch, D. *J. Phys. Chem. B* **1997**, *101*, 1279.  
(10) Bakir, M.; Sullivan, B. P.; Mackay, S. G.; Linton, R. W.; Meyer, T. J. *Chem. Mater.* **1996**, *8*, 2461.

particle morphology, resulting in nonuniform particle formation. Since nanoparticle size can have a dramatic effect on material properties, controllable narrow size distribution is a primary goal of modern nanoparticle preparation techniques. This problem can be alleviated if a nanostructured polymeric matrix could be employed to regulate the extent of metal nanoparticle formation. Excellent examples of well-defined nanoscale polymer matrixes are micelles formed by block copolymer molecules in selective solvent(s). In this case, the micelles serve as "nanoreactors" for highly controlled nanoparticle preparation.<sup>13–16</sup> Recent efforts<sup>17–19</sup> have likewise used the microdomains of microphase-separated block copolymers to control nanoparticle growth without the use of solvent(s).

Since the synthesis of some well-defined block copolymers can be complicated and the molecular characteristics and phase behavior of copolymers are intimately coupled, use of simple homopolymer matrixes to prepare nanoparticles with a narrow size distribution may be technologically preferable. To achieve this, a given polymer network must possess either a high degree of cross-linking (to restrict the size of growing nanoparticles) or functional groups that stabilize the nanoparticles. Antonietti et al.<sup>20</sup> have recently reported that the size of gold nanoparticles could be controlled in sulfonated polystyrene *microgels*, which are nanoscale cross-linked polymer gels. An example of a highly cross-linked polymeric matrix designed for the production of Cr nanoparticles is derived<sup>21</sup> from poly(1,4-phenylene)silsesquioxane. Formation of Cr nanoparticles within matrix pores measuring 4–5 nm in diameter requires cocondensation of the corresponding trifunctional monomer with an organometallic precursor, a Cr<sup>0</sup> species bound to phenyl rings. Thermolysis of intermediate Cr arenes yields nanoparticles residing in the pores of the polymer matrix, but possessing a broad size distribution despite the relatively low Cr content (0.68 wt %).

The present work reports on the use of hyper-cross-linked polystyrene (HPS)<sup>22</sup> as a matrix material for the controlled formation of Co nanoparticles. Due to the high cross-linking density achievable, HPS is expected to consist of nanosized rigid cavities of comparable size. Moreover, a unique feature of HPS is its ability to swell in numerous solvents, even in thermodynamically poor ones, thereby facilitating incorporation of a wide range of organometallic compounds into the matrix. In this

work, we seek to ascertain if the cavities of HPS can serve to restrict metal particle growth and provide a fine control of particle size and shape. Cobalt nanoparticles are selected since their size characteristics can be discerned<sup>4</sup> by ferromagnetic resonance (FMR) spectroscopy.

## Experimental Section

**Materials.** Styrene–divinylbenzene (DVB) copolymer (0.7 wt % divinylbenzene) was obtained by common suspension copolymerization.

Technical grade monochlorodimethyl ether (MCDE) was distilled taking the fraction with boiling temperature of 57–61 °C.

Hyper-cross-linked polymer was prepared by cross-linking the styrene–DVB copolymer, swollen in anhydrous ethylene dichloride, with MCDE in the presence of FeCl<sub>3</sub> as catalyst. The molar ratio of the components was 1:1:0.3, respectively. The reaction was carried out at 80 °C for 10 h. In the presence of a catalyst, the cross-linking agent was completely consumed and converted mainly into –CH<sub>2</sub>– bridges. The polymer obtained was washed with acetone, 0.5 N HCl, and water. The excess of water was filtered out and the polymer was placed in an excess of a solution of 15% NaOH in methanol to convert some semireacted CH<sub>2</sub>OH groups to CH<sub>2</sub>OCH<sub>3</sub> groups. The beads were agitated at 60 °C for 8 h. Finally, the product was washed with water and dried at 60 °C overnight.

The apparent specific surface area of the resulting HPS was measured by the standard Ar desorption method. All the HPS samples were proved to be microporous products.<sup>22,23</sup> For HPS prepared by a procedure similar to the one described above, pore size distribution was estimated from both N<sub>2</sub> adsorption isotherms and size exclusion chromatography data.<sup>23</sup>

The organometallic precursor, Co<sub>2</sub>(CO)<sub>8</sub>, as well as the solvents dimethylformamide (DMF) and 2-propanol, were purchased from Fluka. Solvents were used as received, whereas the Co<sub>2</sub>(CO)<sub>8</sub> was purified by crystallization from pentane. Two delivery systems were utilized in this work to introduce Co into the HPS matrix: (I) Co<sub>2</sub>(CO)<sub>8</sub> in 2-propanol solution and (II) the cationic–anionic complex [Co(DMF)<sub>6</sub>]<sup>2+</sup>[Co(CO)<sub>4</sub>]<sup>2-</sup> produced in situ upon dissociation of Co<sub>2</sub>(CO)<sub>8</sub> in DMF.<sup>4</sup>

**Methods.** Solutions I and II were prepared in Shlenk tubes equipped with magnetic stir bars and held under pure Ar. A predetermined amount (ca. 1 g) of HPS was evacuated in a Shlenk tube and likewise filled with Ar, and a preselected quantity (ca. 2.6 mL) of solution I or II was injected by syringe, through rubber septum, into the HPS to ensure complete polymer swelling without excess solution. Once the HPS was fully swollen (over the course of about 30 min), the solvent was evaporated in vacuo (1.50 mbar) for 3 days. To increase the Co content in a given sample, several successive sorptions were performed. A fraction of each dried Co-containing specimen was thermolyzed in vacuo (1.33·10<sup>-5</sup> mbar) at 200 °C for several hours in a glass ampule, which was subsequently heat-sealed.

After thermolysis, each sample was examined by XRF and FMR spectroscopies. The Co content of each specimen was deduced from XRF measurements, performed on a Zeiss Jena VRA-30 spectrometer equipped with an Mo anode, LiF crystal analyzer, and SZ detector. Analyses were based on the Co K $\alpha$  line and a series of standards prepared by mixing 1 g of polystyrene with 10–20 mg of standard compounds. The time of data acquisition was held constant at 10 s. The FMR analyses were conducted at 25 °C with a Varian E-12 spectrometer on the HPS–Co powder in each sealed ampule. Transmission electron microscopy was performed on three samples to discern the size distribution of Co nanoparticles. Insoluble HPS–Co powders were embedded in epoxy resin. Upon completion of resin cure, the embedded powders were

(11) Kroll, E.; Winnik, F. M.; Ziolo, R. F. *Chem. Mater.* **1996**, *8*, 1594.

(12) Weaver, S.; Taylor, D.; Gale, W.; Mills, G. *Langmuir* **1996**, *12*, 4618.

(13) Antonietti, M.; Wenz, E.; Bronstein, L. M.; Seregina, M. S. *Adv. Mater.* **1995**, *7*, 1000.

(14) Platonova, O. A.; Bronstein, L. M.; Solodovnikov, S. P.; Yanovskaya, I. M.; Obolonkova, E. S.; Valetsky, P. M.; Wenz, E.; Antonietti, M. *Colloid Polym. Sci.* **1997**, *275*, 426.

(15) Spatz, J. P.; Roescher, A.; Möller, M. *Adv. Mater.* **1996**, *8*, 337.

(16) Bronstein, L. M.; Sidorov, S. N.; Gourkova, A. Y.; Valetsky, P. M.; Hartmann, J.; Breulmann, M.; Cölfen, H.; Antonietti, M. *Inorg. Chim. Acta* **1998**, *280*, 348.

(17) Möller, M. *Synth. Met.* **1991**, *41–43*, 1159.

(18) Sohn, B. H.; Cohen, R. E. *J. Appl. Polym. Sci.* **1997**, *65*, 723.

(19) Ciebien, J. F.; Clay, R. T.; Sohn, B. H.; Cohen, R. E. *New J. Chem.* **1998**, 685.

(20) Antonietti, M.; Gröhn, F.; Hartmann, J.; Bronstein, L. *Angew. Chem. (Int. Ed. Engl.)* **1997**, *36*, 2080.

(21) Choi, K. M.; Shea, K. J. *J. Am. Chem. Soc.* **1994**, *116*, 9052.

(22) Davankov, V. A.; Tsyurupa, M. P. *Reactive Polym.* **1990**, *13*, 27.

(23) Tsyurupa, M. P.; Davankov, V. A. *J. Polym. Sci.: Polym. Phys. Ed.* **1980**, *18*, 1399.

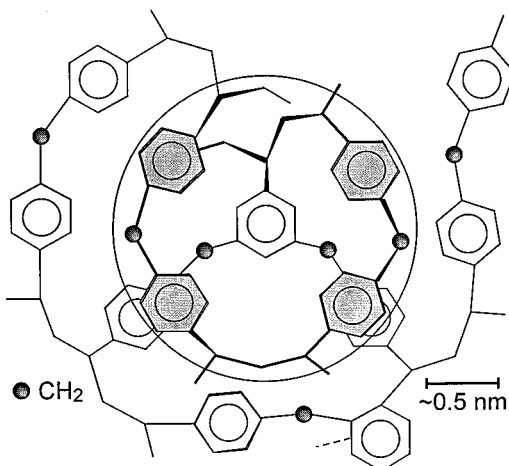


**Figure 1.** Schematic illustration of the internal network of hyper-cross-linked polystyrene (HPS). The speckled phenyl rings reside in a different plane relative to the unspeckled ones in the cross-linked material, and the circle identifies a postulated cavity in which Co nanoparticles could grow.

microtomed at ambient temperature, and the resulting thin sections (ca. 50 nm thick) were imaged with a Zeiss EM902 electron spectroscopic microscope operated at 80 kV and an energy loss of 0 eV. Negatives were digitized at 600 dpi, and the resulting digital images were analyzed with the NIH Image software package.

## Results and Discussion

**Justification of Selections.** Hyper-cross-linked polystyrene constitutes the first representative of a novel class of polymer networks<sup>22</sup> and is distinguished by a unique topology and an unusual set of properties. Two basic conditions must be met in order to obtain a *hyper*-cross-linked network. First, the material must be prepared in the presence of a good solvent (i) to prevent any degree of phase separation and (ii) to obtain an open network microstructure. Second, the final network must be conformationally rigid to preclude the possibility of collapse upon removal of the synthesis solvent. Thus, HPS can be prepared by introducing numerous  $-\text{CH}_2-$  bridges between adjacent phenyl rings of linear polystyrene or poly(styrene-*r*-divinylbenzene) copolymer chains that exist either in solution or as swollen gel beads, respectively, in the presence of ethylene dichloride. Monochlorodimethyl ether or dimethyl formal are generally employed as bifunctional cross-linking agents for styrene and divinylbenzene in the presence of a Friedel-Crafts catalyst. To obtain a rigid network structure, the degree of cross-linking for polystyrene must be high, at least 40%. In practice, it can exceed 100% when all the phenyl rings of the initial polystyrene are involved in the formation of cross-link sites. A schematic illustration of the network microstructure envisioned in HPS is presented in Figure 1.

Rigid hyper-cross-linked polymers exhibit extremely high inner surface area, typically in the range of 1000  $\text{m}^2/\text{g}$ , as well as the peculiar property to swell nonselectively (i.e., to increase in volume in the presence of any type of liquid media, including known precipitators of the parent polymer). In the present study, the HPS used as the matrix for Co nanoparticle formation has been found to exhibit the following characteristics: (a) formal degree of cross-linking of 200%, (b) apparent

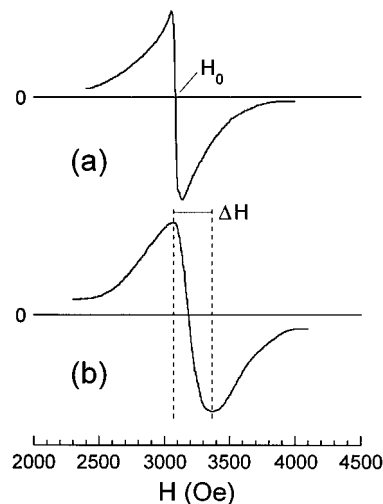


**Figure 2.** FMR spectra of the HPS-Co specimens containing (a) 5.07 and (b) 10.08 wt % Co and obtained by thermolysis at 200 °C for 2 h. Labeled in panel a is the definition of  $H_0$ , the magnitude of which is related to the shape of the Co nanoparticles. The vertical dash lines in panel b identify the line width corresponding to  $\Delta H$ , which provides a measure of particle size.

inner surface area of 833  $\text{m}^2/\text{g}$ , (c) pore size at about 2–3 nm in diameter, and (d) particle sizes ranging from 0.2 to 0.4 nm.

Cobalt nanoparticles have been selected here due to the established<sup>24</sup> correlation between size and shape of Co particles and their magnetic properties, i.e., their FMR spectrum characteristics. Particles measuring less than 1 nm in diameter are nonmagnetic, while those with diameters from 1 to 10 nm are superparamagnetic. Larger Co particles behave as ferromagnetic materials. Moreover, the width of the FMR signal ( $\Delta H$ ) for spherical particles depends on the size of the Co nanoparticles,<sup>24,25</sup> and the position corresponding to the zero signal ( $H_0$ ) contains information regarding the shape of the Co nanoparticles.<sup>24</sup> This allows one to discern the general size and shape characteristics of Co nanoparticles solely from FMR spectra.

Selection of one of the nanoparticle processing conditions, namely, the thermolysis temperature, also warrants mention here. Specimens produced at temperatures in the range of 100–120 °C do not exhibit a FMR signal, suggesting that the Co nanoparticles, if any form, exist as magnetically disordered entities less than 1 nm in diameter. At temperatures above 220 °C, thermal restructuring of the HPS network has been observed<sup>26</sup> to occur. Therefore, an intermediate temperature (200 °C) has been chosen to maximize the degree of magnetic order in Co nanoparticles measuring larger than 1 nm in diameter, without damaging the HPS matrix.

**Characterization of Nanoparticles.** Shown in Figure 2 are representative FMR spectra of HPS-Co composites prepared from  $[\text{Co}(\text{DMF})_6]^{2+}[\text{Co}(\text{CO})_4]^{-2}$  in DMF with 5.07 (Figure 2a) and 10.08 (Figure 2b) wt % Co. The definitions of  $H_0$  and  $\Delta H$  mentioned in the previous section are illustrated in these figures for the

(24) Vonsovskii, S. V. *Magnetism*; Nauka: Moscow, 1971.

(25) Bean, C. P.; Livingston, J. D.; Rodbell, P. S. *Acta Metall.* **1957**, *5*, 682.

(26) Pastukhov, A. V.; Tsyurupa, M. P.; Davankov, V. A. *J. Polym. Sci. B: Polym. Phys.* Submitted.

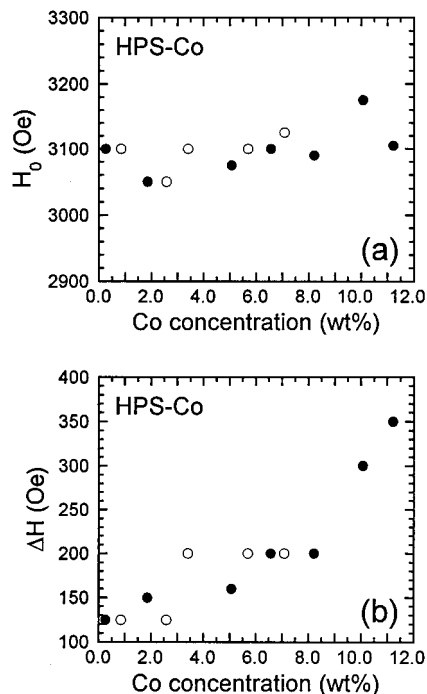


**Figure 3.** Concentration dependence of (a)  $H_0$  and (b)  $\Delta H$  derived from FMR spectra (see Figure 2 for definitions) for HPS-Co composites produced from  $\text{Co}_2(\text{CO})_8$  in 2-propanol (○) and  $[\text{Co}(\text{DMF})_6]^{2+}[\text{Co}(\text{CO})_4]^{-2}$  in DMF (●) at 200 °C for 2 h.

sake of clarity. Values of  $H_0$  and  $\Delta H$  derived from FMR spectra of HPS-Co composites prepared from the two Co carbonyl compounds described in the Experimental Section are displayed as a function of Co concentration in parts a and b of Figure 3, respectively. Two important features are evident from the data shown in Figure 3a: (i) an increase in Co content up to about 11 wt % does not noticeably affect the magnitude of  $H_0$  ( $\pm 30$  Oe), and (ii)  $H_0$  appears to be independent of the precursor organometallic compound. It should be noticed that the value of  $H_0$  provides evidence for spherical particle formation varying in the range from 2900 to 3200 Oe,<sup>24</sup> which was also discussed in our earlier publication.<sup>14</sup> All of the nanoparticles examined here are therefore presumed to possess a spherical morphology. Values of  $\Delta H$  in Figure 3b and, hence, nanoparticle sizes are nearly independent of the Co precursor employed. Indeed, because  $\Delta H$  is a very sensitive parameter, variation of its value within  $\pm 50$  Oe is the accuracy of the Co particle size determination.<sup>24</sup> Comparison of the magnitudes of the FMR line widths shown in Figure 3b with data published elsewhere<sup>25,27</sup> reveals that the Co nanoparticles formed in HPS at Co loadings from about 2 up to about 8 wt % ( $\Delta H = 150\text{--}200$  Oe) measure on the order of 2 nm in diameter. At lower loadings particles appear to be smaller. When the Co content exceeds ca. 8 wt %, the concentration dependence of the FMR line width becomes really pronounced. The line width acquired from the HPS-Co composite with 11 wt % Co (at  $\Delta H = 350$  Oe) signals an increase in nanoparticle diameter of about 1 nm.<sup>24</sup>

According to the data in Table 1, the thermolysis duration at 200 °C has little impact on the FMR

**Table 1.** FMR Data of HPS-Co Samples Thermolyzed at 200 °C and Various Durations

Co content (wt %)	time of thermolysis (h)	$H_0$ (Oe)	$\Delta H$ (Oe)
$\text{Co}_2(\text{CO})_8$ in 2-propanol			
0.9	2	3115	170
0.9	6	3100	250
3.0	2	3040	200
3.0	6	3050	200
3.0	10	3035	200
$[\text{Co}(\text{DMF})_6]^{2+}[\text{Co}(\text{CO})_4]^{-2}$ in DMF			
1.2	2	3100	200
1.2	6	3050	200
1.2	10	3060	220

parameters  $H_0$  and  $\Delta H$ , thereby ensuring that the Co nanoparticles do not agglomerate during the prolonged heating at this temperature. Negligible nanoparticle agglomeration under these conditions provides evidence that the HPS network is stable and does not restructure to a noticeable extent, at 200 °C. The data in Table 1 also demonstrate that the organometallic compound used to prepare the Co nanoparticles has little effect on the size and shape of the resultant nanoparticles. Thus, over a relatively large range of Co concentrations (from 2.0 to 8.0 wt %), the polymeric matrix appears to exert considerable control over nanoparticle growth, yielding nanoparticles with nearly identical sizes and shape, independent of the metal precursor or thermolysis duration. Combining the data in Figure 3 and Table 1 clearly demonstrates that the HPS route for highly controlled nanoparticle production is robust.

The FMR data shown in Figures 2 and 3 and listed in Table 1 provide only approximate mean particle sizes. To investigate the Co nanoparticle morphology in greater detail, TEM has been performed on the same samples whose FMR spectra are displayed in Figure 2. Shown in Figure 4 are TEM images from the neat HPS matrix (Figure 4a), as well as the HPS-Co composites with 5.07 (Figure 4b) and 10.08 (Figure 4c) wt % Co. In these zero-loss images, which utilize only unscattered and inelastically scattered electrons during acquisition, the Co nanoparticles appear as electron opaque (dark) dots due to their high electron density relative to the HPS background. Comparison of part a with parts b and c of Figure 4 confirms that the nanoparticles only exist in the two specimens containing Co. Direct visualization of the ca. 2 nm pores comprising the HPS network microstructure is not, however, possible from images such as these due to insufficient phase contrast from sections measuring ca. 50 nm thick (approximately 25 Å the diameter of a pore).

Stereological analysis of several images such as those presented in Figure 4 yields the particle-size histograms displayed in parts a (5.07 wt % Co) and b (10.08 wt % Co) of Figure 5. No Co nanoparticles less than ca. 1 nm across are clearly discernible in any of the images due, in part, to the resolution of the microscope (estimated to be about 0.5 nm). An interesting feature of both histograms is that the median particle size lies between 2 and 3 nm, in excellent agreement with the particle size inferences from the FMR data. In fact, the mean diameter of the Co nanoparticles in the HPS-Co specimen with 5.07 wt % Co is  $2.88 \pm 1.31$  nm. As the concentration of Co is nearly doubled to 10.08 wt %, the population of large particles (some measuring up to 15

(27) Kuznetsov, V. L.; Lisitsyn, A. S.; Golovin, A. V.; Aleksandrov, M. N.; Yermakov, Yu. I. In *Fifth International Symposium: Homogeneous and Heterogeneous Catalysis*; Coronet: Novosibirsk, 1986; p 83.

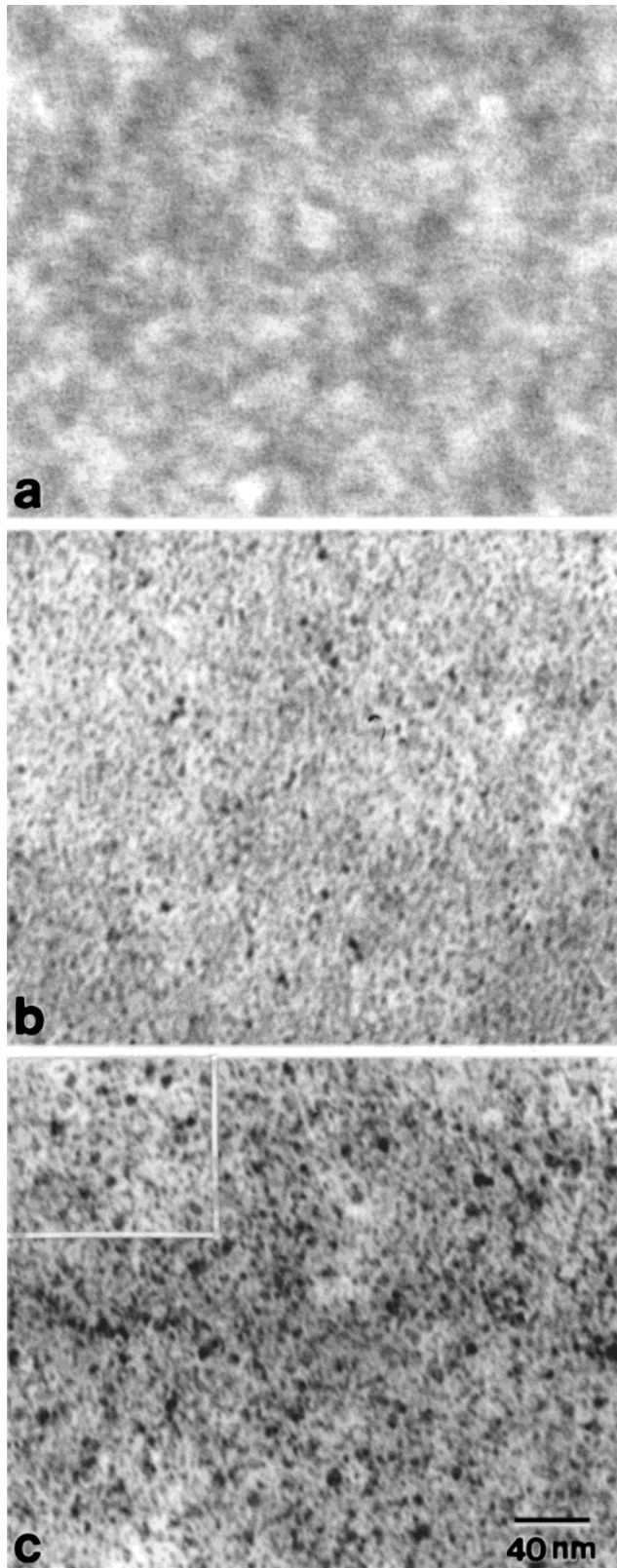


**Figure 4.** TEM micrographs of (a) unmodified HPS, as well as the HPS-Co specimens containing (b) 5.07 wt % Co and (c) 10.08 wt % Co and obtained by thermolysis at 200 °C for 2 h. The inset in panel c more clearly shows the nanoparticles in a thin region of the ultramicrotomed specimen.

nm in diameter) increases, thereby shifting the mean particle diameter to  $3.69 \pm 2.26$  nm.

The histograms in Figure 5a,b treat the Co nanoparticles as equivalent spheres (circles in projection), and

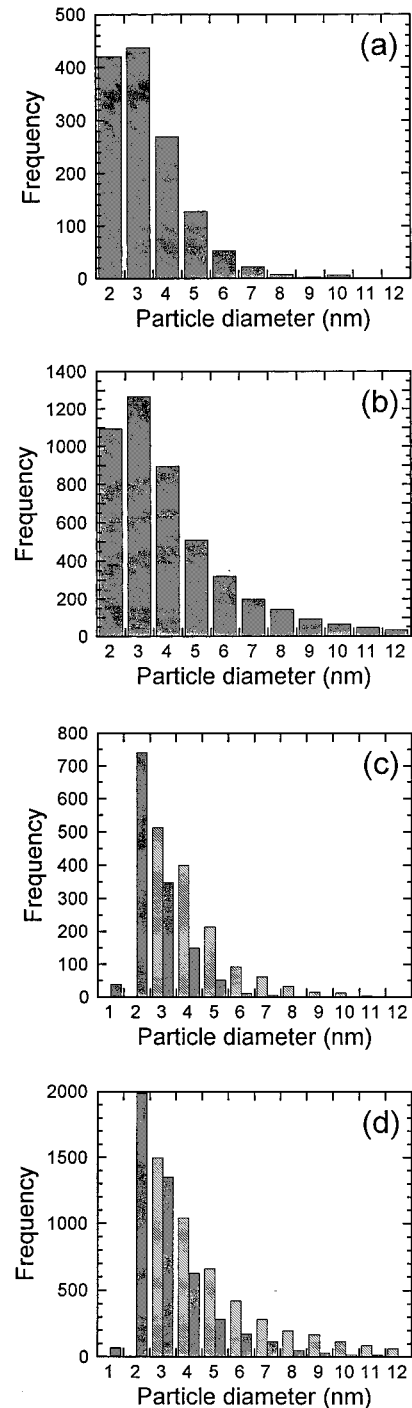


**Figure 5.** Histograms of the particle size distributions obtained from TEM images such as those presented in Figure 4. The data in parts a and c refer to the HPS-Co composite possessing 5.07 wt % Co, while those in b and d correspond to the material with 10.08 wt % Co. Histograms in parts a and b treat the particles as circles in projection, whereas those in c and d consider the particles as ellipses with major (darker bars) and minor (lighter bars) axes in projection.

do not consider particle asphericity or overlap. While particle asphericity is not considered to be a major source of bias in light of the FMR data presented earlier, the overlap of 2–3 nm particles in projection through ca. 50 nm sections can constitute a nonnegligible source of error. By treating the Co nanoparticles as ellipsoids (ellipses in projection), rather than spheres, decoupled measurements of the major and minor axes of each

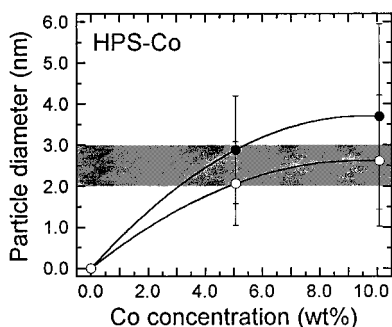


**Figure 6.** Variation of mean nanoparticle diameter with Co concentration, as discerned from TEM images in which the particles are treated as spheres (●) or ellipses (○), with only the minor axis shown. The crosshatched region identifies the size range from FMR spectroscopy, and the vertical lines denote one standard deviation in the TEM data. The solid lines serve as guides for the eye.

nanoparticle can be ascertained and the corresponding histograms generated: parts c (5.07 wt % Co) and d (10.08 wt % Co) of Figure 5. Comparison of all the histograms in Figure 5 reveals nontrivial deviation from sphericity by many of the particles included in the population sampling. Since the Co nanoparticles are presumed to be spheroidal in nature (so that any apparent asphericity can be attributed solely to particle overlap), we need only consider further the average measurements of the particles' minor axis:  $2.06 \pm 1.02$  and  $2.61 \pm 1.59$  nm for the HPS-Co specimens with 5.07 and 10.08 wt %, respectively. To put the population of particles within this size regime in perspective, particles larger than 3 nm in diameter account for about 16% of the nanoparticles in the composite with 5.07 wt % Co, but 28% in the specimen with 10.08 wt % Co. To summarize these findings, we present the mean Co nanoparticle diameters derived from TEM images as a function of Co content in Figure 6.

On the basis of the data presented here, the nanoscale HPS network is deemed responsible for controlling Co nanoparticle formation. In many instances, nanoparticle size is governed by rates of nucleation and growth. If this were true here, the nucleation of Co nanoparticles must be strongly dependent on thermolysis temperature/duration and Co precursor type. The cationic-anionic complex  $[\text{Co}(\text{DMF})_6]^{2+}[\text{Co}(\text{CO})_4]^{-2}$  is found<sup>4</sup> to be more thermally stable than  $\text{Co}_2(\text{CO})_8$ , decomposing at 110 °C compared to ambient temperature for cobalt octacarbonyl.<sup>28</sup> Since the decomposition of the two Co precursors occurs at 200 °C in the present work, a difference in thermal stability most likely does not

influence the nucleation rate of Co nanoparticles. Thus, it seems reasonable to suspect that, despite differences in thermolysis duration, nucleation transpires at nearly the same rate in all the specimens examined here.

This dilemma suggests that another consideration limits Co nanoparticle growth. The HPS employed here does not contain functional groups that could specifically interact with, and stabilize, growing metal nanoparticles. In fact, the nanoscale cavities envisioned in HPS (see Figure 1) are anticipated to be highly interconnected and, therefore, should *not* hinder the migration of Co atoms or even small Co clusters. A steric limitation arising from the preponderance of phenyl rings, which could serve to interact with metal surfaces and nonspecifically stabilize metal nanoparticles, appears to represent the most probable reason for controlled Co nanoparticle growth in HPS. If the Co concentration in a HPS-Co composite exceeds a saturation limit (at Co loadings in excess of 10 wt %), a few large nanoparticles grow. Their size might (i) correlate with the statistics of the pore size distribution of the HPS matrix or (ii) identify a metal-induced rearrangement of the HPS network. Further study of the growth mechanism of nanoparticles in HPS is clearly warranted.

### Conclusions

This study focuses on a relatively simple alternative by which to prepare highly dispersed hybrid composites derived from hyper-cross-linked polystyrene, which contains nanoscale cavities or pores within conformationally rigid structures. Such cavities serve as nanoreactors in which various Co carbonyl complexes are consumed and Co nanoparticle growth (expressed in terms of particle size and size distribution) is physically controlled by the polymeric matrix during the thermolysis of different Co organometallic compounds in a wide range of Co contents (2–8 wt %). Nanoparticle size estimates obtained from FMR and TEM are in excellent agreement, and they demonstrate that the mean nanoparticle size is surprisingly comparable to the average pore size of the polymeric matrix.

**Acknowledgment.** L.M.B., S.N.S., and P.M.V. acknowledge financial support provided by the Russian Foundation for Basic Research (Grant No. 98-03-33372). V.A.D. and M.P.T. are grateful for financial support from the Civil Research and Development Foundation (Grant RC 1-179). E.A.W. and R.J.S. thank Milliken Chemicals and, in part, the National Science Foundation (CMS 941-2361) for the financial support and Mr. A. P. Smith for technical assistance.

CM990274P

(28) Wilkinson, G. *Comprehensive Organometallic Chemistry: The Synthesis, Reactions and Structures of Organometallic Compounds*; Pergamon: New York, 1982.